nanomaterials

MDPI

Article

Conditions for production of composite material based on aluminum and carbon nanofibers (CNFs) and its physic-mechanical properties

Oleg V. Tolochko[1], Tatiana S. Koltsova[1], Elizaveta V. Bobrynina[1], Andrei I. Rudskoy[1], Elena G. Zemtsova [2], Sergey O. Kirichenko[2], Vladimir M. Smirnov[2]

[1] Peter the Great St.Petersburg Polytechnic University, Polytechnicheskaya 29, 195251, St.Petersburg, Russia; ol_tol@hotmail.com (O.V.T.); annelet@yandex.ru (T.S.K.)

[2] Saint Petersburg State University, Universitetskii pr.26, 198504, Saint Petersburg, Russia; vms11@yandex.ru V.M.S.)

Received: 23 November 2018; Accepted: 2018; Published: 2018

Abstract: Aluminum-based metallic matrix composites reinforced by carbon nanofibers (CNF) are important precursors for development of new light and ultralight materials with enhanced properties and high specific characteristics. In the present work, powder metallurgy technique was applied for production of composites based on reinforcement of aluminum matrices by CNFs of different concentrations (0~2.5 weight%). CNFs were produced by chemical vapor deposition (CVD) and mechanical activation. We determined that *in situ* synthesis of carbon nanostructures with subsequent mechanic activation provides satisfactory distribution of nanofibers and homogeneous composite microstructure. Introduction of 1 vol% of flux (0.25 NaCl + 0.25 KCl + 0.5 CaF_2) during mechanic activation helps to reduce the strength of the contacts between the particles. Also, better reinforcement of alumina particles and strengthening the bond between CNFs and aluminum are observed due to alumina film removal. Introduction of pure aluminum into mechanically alloyed powder provides the possibility to control composite durability, plasticity and thermal conductivity.

Keywords: composite; metallic matrix**;** aluminum; powder; surface; pressing; dispersed phase, carbon nanofibers; durability; thermal conductivity

1. Introduction

In many areas, particularly in the aerospace and automotive industries, the replacement of steel with light and ultra-light composites results in reduced weight and improved fuel efficiency. Industry needs to further reduce the vehicles weight while maintaining their structural integrity and safety. This explains a great interest in the creation of composites for complex structural components. This trend will undoubtedly continue in the 21st century, as the transport sector of the economy needs a global search for ways to reduce CO_2 emissions.

From this point of view, the strategic area of material chemistry is development of synthetic works to gain light and ultralight composites with improved properties and high specific characteristics.

Recently, metal matrix composites reinforced with carbon nanotubes (CNTs) and carbon nanofibers (CNFs) became the subject of many studies [1]. This is due to the unique properties of CNTs, e.g. the strength of up to 63 GPa [2] and the thermal conductivity of 3000 W/m·K [3]. Uniform distribution of carbon nanotubes in the metal matrix remains a challenge due to their high propensity for agglomeration. There are the attempts to solve the problem on the composite preparation stage and on compaction stage [1]. Most traditional methods of mixing of the matrix and CNTs powders are a mechanical grinding in a ball mill [4–8], flake powder metallurgy [9, 10] molecular level mixing [11], *in situ* CNT growth on metal powders [12-14] and spray drying of small metal particles with CNTs [15].

To create metal-based compact materials reinforced by CNTs, technologies of powder metallurgy [16, 17], liquid metallurgy [18], galvanic plating [19], sintering in spark plasma [20, 21], and thermal spraying are used [22, 23].

Significant problem here is the difficulty to reach a balance between strength and ductility for Al-CNT composites. If the enhanced tensile strength was obtained by addition of CNTs then the ductility of composites was low [24–25]. This effect is attributed to the difficulties in achieving metal-CNT composites with uniform CNTs dispersion in the matrix and the strong interfacial bonding between the CNTs and the Al matrix.

In the current paper, we investigate the possibility to produce the aluminum-based composites reinforced with carbon nanostructures with different CNT content (0~2.5 wt.%) by powder metallurgy and mechanical activation. Carbon nanostructures were obtained by chemical vapor deposition (CVD) directly onto matrix aluminum particles (*in situ*) with subsequent milling of composite in planetary ball mill. We expected that such approach leads to uniform distribution of dispersed phase CNFs) in aluminum matrix along with strong bond between CNF and aluminum matrix phases.

2. Materials and Methods

2.1. Materials

The initial material used was pulverized aluminum powder of PA-4 mark, GOST 6058-73 standard with particle size less than 120 μm and purity of 99.5 wt.%. Amounts of the main impurities (Si, Fe, Cu) do not exceed 0.4, 0.35 and 0.02 wt.%, respectively.

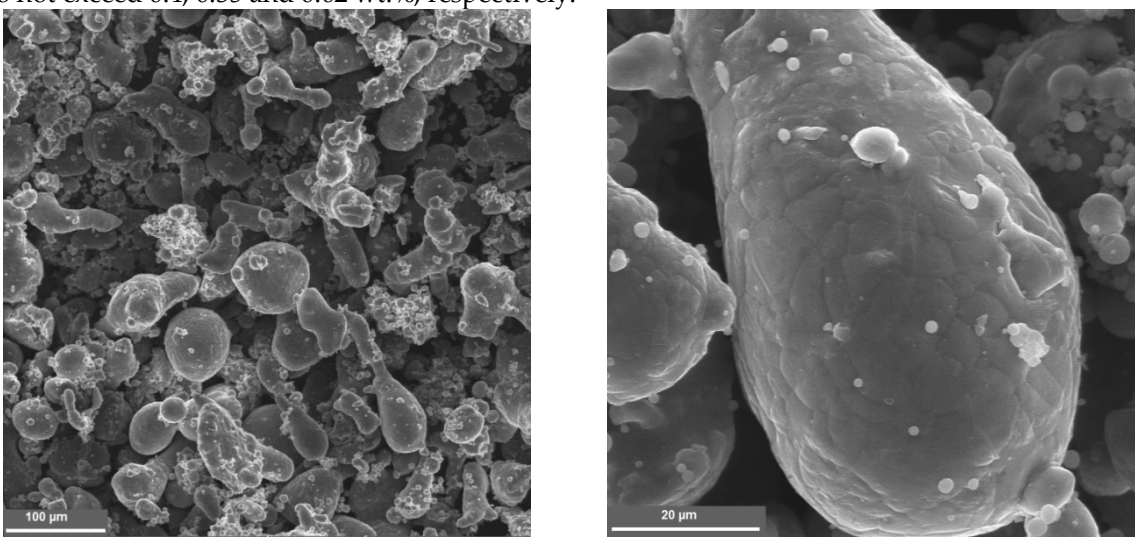

(**a**) (**b**)

Figure 1. Microstructure of the composite particle.

The powder particles had a teardrop shape and a rough surface (Figure 1).

2.2. Preparation of aluminum-CNFs composites

To grow carbon nanostructures, a nickel- or cobalt-containing catalyst with 0.035 wt.% Ni or Co was deposited on the powder surface. The metal source was either $Ni(NO_3)_2 \cdot 6H_2O$ or $Co(NO_3)_2 \cdot 6H_2O$ that are highly soluble in water and decompose to NiO and CoO at 300–350°C. The aluminum powder was mixed with a 0.01% aqueous solution of Ni or Co nitrate (10 ml per 1 g powder). The solution was stirred for 10 min and then carefully dried at 100°C in a drying chamber. Then the powder was heated additionally in a hydrogen atmosphere for complete reduction of salts to metallic nickel or cobalt. The reactor was blown with argon before and after the synthesis (flow rate of 200 ml/min). H_2/C_2H_2 ratio in the gas mixture during the synthesis was 8.31. The temperature of the synthesis was 550°C.

Mechanical activation of the powder was carried out in a micro-mill PULVERISETTE 7 premium line. The 2.5 wt.%-Al-CNTs composite powders (with the addition of 1 vol.% flux 0.25 NaCl + 0.25 KCl +

0.5 CaF_2) were placed in 80 ml stainless steel jars containing stainless steel balls of 10 mm diameter (ball-to-powder ratio = 10:1). The powders were milled under argon at 500 rpm for 180 min. For variation of CNFs content, the mechanically activated Al-CNFs samples were mixed with a certain amounts of pure Al powder at 500 rpm for 180 min.

2.3. Powder compaction

The specimens were compacted by the cold pressing at a pressure of 800 MPa with subsequent heating with mold up to 480 °C with final hot pressing at 600 MPa.

2.4. Characterization

The structure and morphology of the powder materials was studied by scanning electron microscopy (TESCAN Mira-3M).

Metallographic studies were carried out using an optical microscope (Carl Zeiss Observer D1m). The thermal conductivity of the specimens was computed from the measured values of the thermal diffusivity by an equation:

$$\lambda = \alpha \varrho c_p, \quad (1)$$

where c_p [J(g·K)] is the specific heat capacity of the specimen. The accuracy of the measurements was 2.3% for the thermal diffusivity, 4% for the heat capacity, and 5% for the thermal conductivity.

The density of the sintered specimens was determined by hydrostatic weighing.

2.5. Mechanical tests

Brinell hardness (HB) was tested using a hard alloy ball 5 mm in diameter at a load of 98 N. Bending tests were carried out in accordance with GOST 14019-80 "Metals and alloys. Methods of testing for bending".

2.6. Specific surface area and porosity measurement

Specific surface area was calculated from physical adsorption data that obtained using volumetric analyzer-porometer Micromeritics ASAP2020 MP. Preliminary adsorption isotherms measurements were carried out using standard nitrogen adsorption technique at 77 K; specific surface areas were calculated by BET and total pore volumes, available for adsorption (so called Gurvich volume) at relative pressure of 0.995. Due to the small specific surface area of the samples, additional measurements using krypton as an adsorbate were carried out at 77 K to clarify the values of specific surfaces, the specific surface was calculated using BET. Before tests, the specimens were vacuum degassed at 250°C for at least 14 h.

2.7. Raman spectral studies

Raman spectra were recorded using Raman spectrometer Bruker Senterra T64000 with excitation wavelength of 488 nm in the range 100-3500 cm^{-1} Spectra were normalized using SVN technique with subsequent baseline correction.

3. Results and discussion

Study of the specific surface area and porosity of the initial samples of aluminum with CNT on the surface (Table 1) showed that CNTs assist both surface and porosity increase. Flux introduction leads to decrease of both specific surface area and porosity. It can be explained by the blocking of surface available for adsorbate by flux particles.

Table 1. Specific surface and porosity of aluminum/CNT samples

Specimen	**Specific surface area, m^2/g (BET, Kr, 77 K)**	**Specific surface area, m^2/g (BET, N_2, 77 K)**	**Specific porosity, cm^3/g (Gurvich, N_2, 77 K)**
Al-Ni	0.125	–	–
Al-Ni-1%CNT	3.71	3.58	0.014
Al-Ni-1%CNT+flux	0.42	0.42	0.003
Al-Ni-2%CNT	4.70	4.26	0.023
Al-Ni-3%CNT	5.04	3.85	0.013

Raman spectra of all three specimens of aluminum with CNT-modified surface (Figures 2–4) are characterized by typical peaks for graphite-like materials: G-peak at ca. 1580 cm^{-1} corresponding to intraplanar C-C bonds vibrations and D-peak at ca. 1350 cm^{-1} indicating defects and disorder in carbon nanostructures. Also a wide 2D(G*) peak at 2500-2800 cm^{-1} (two-phonon process of the second order) is also characteristic of graphite-like materials containing sp^2-hybridized carbon.

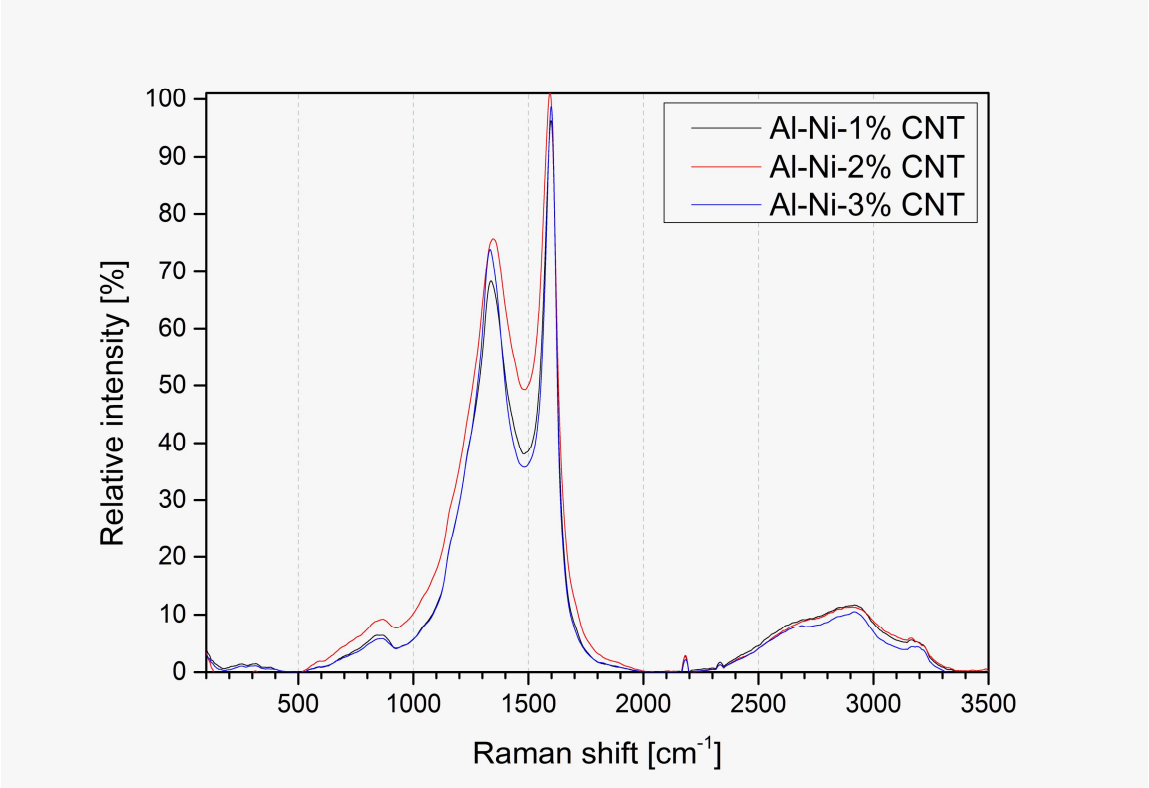

Figure 2. Raman spectra of aluminum with various weight content of CNF

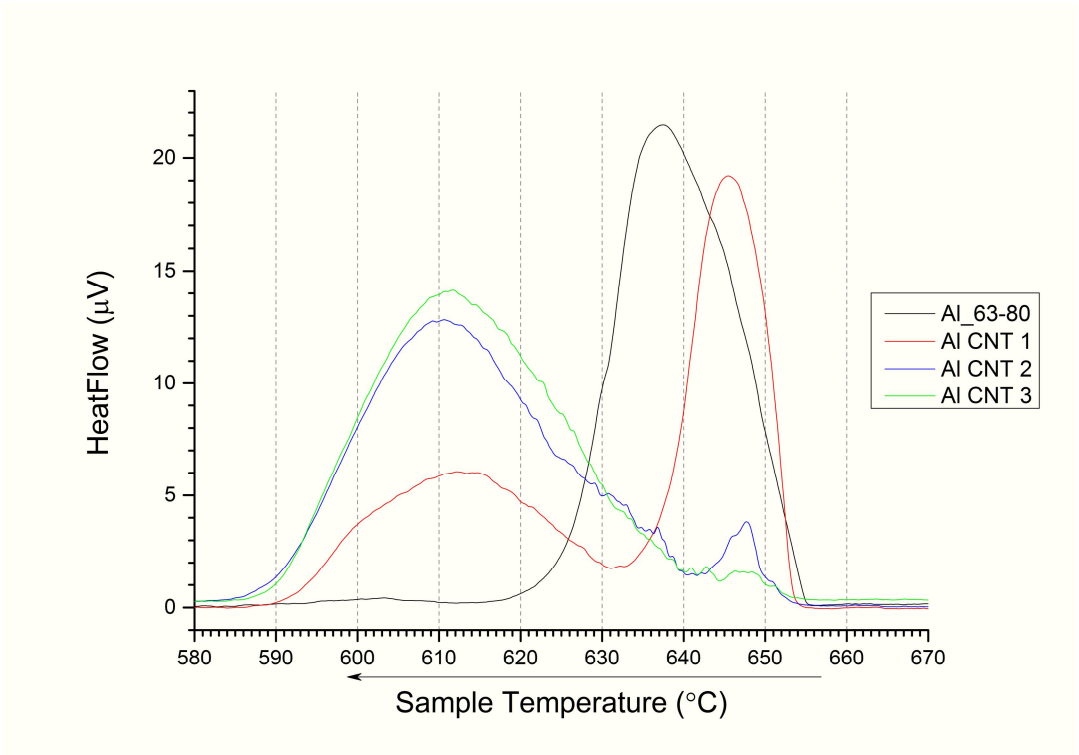

Figure 3. DSC curves of aluminum with various CNF content during cooling near Al melting point

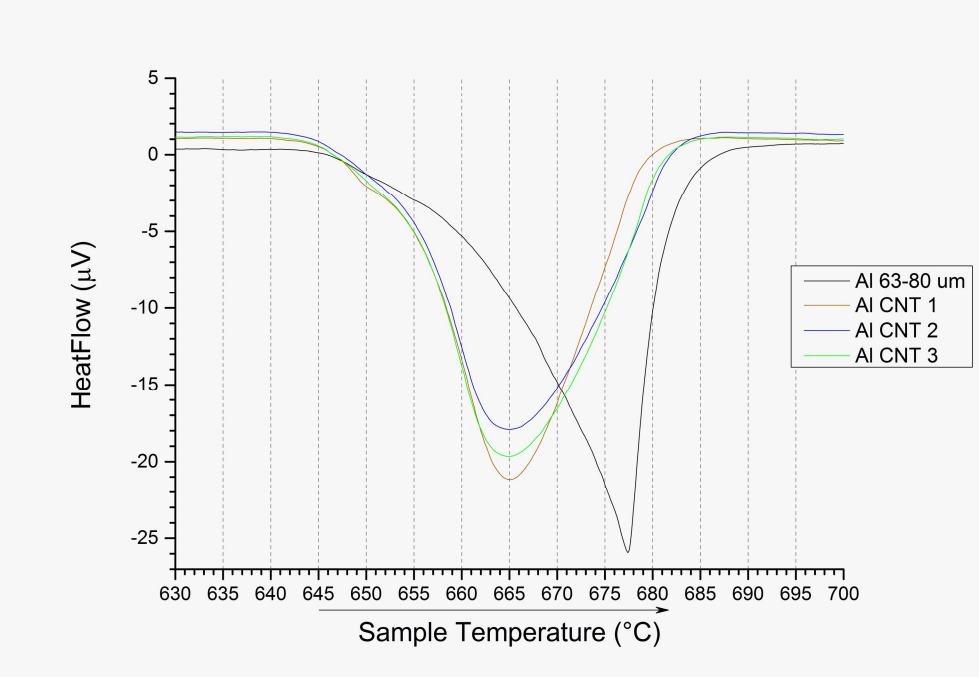

Figure 4. DSC curves of aluminum with various CNF content during heating near Al melting point

To obtain good distribution of carbon nanostructures in the matrix we deposited a nickel and cobalt catalyst onto the surface of the aluminum particles from aqueous solutions. Right before the synthesis, the specimens coated with the catalyst were annealed additionally in a hydrogen environment for 10 min at 550°C to provide decomposition of the nickel or cobalt nitrate and reduction of the oxide to metallic nickel or cobalt that served as catalyst of carbon nanofibers growth on the aluminum powder surface. The content of the metal catalyst was 0.02%.

Carbon nanostructures were synthesized at 550°C for 5–20 min. Figure 5 presents the dependence of the specimen mass variation with respect to the initial weighed portion of aluminum on the synthesis time.

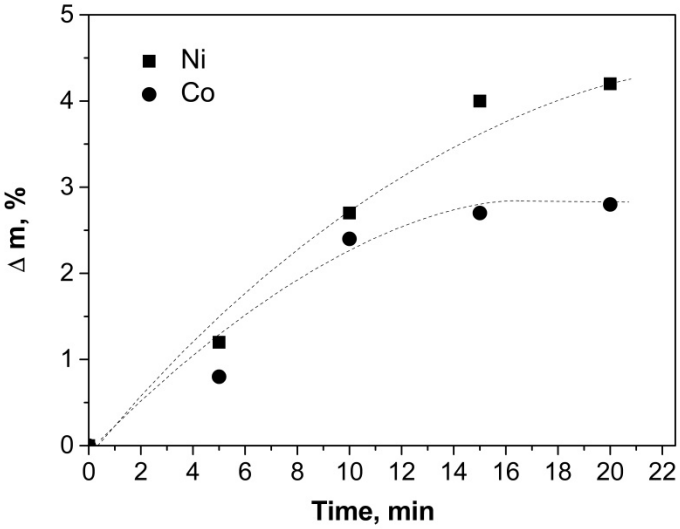

159

160 **Figure 5**. Dependence of the specimen mass variation on the synthesis time at 550°C with Ni and Co catalysts.

161

162 With increase of the synthesis time the growth rate of the carbon nanostructures decreases due to
163 catalyst deactivation, i.e., disappearance of the dominant nucleation places of carbon nanostructures on
164 the powder surface. Nickel catalyst provides a greater amount of carbon. Deactivation of cobalt catalyst
165 occurs faster than nickel one. Rapid deactivation of the catalyst resulted in the production of Co
166 nanofibers with a shorter length. Figure 6 shows SEM images of synthesized aluminum-carbon
167 nanofibers composites.
168

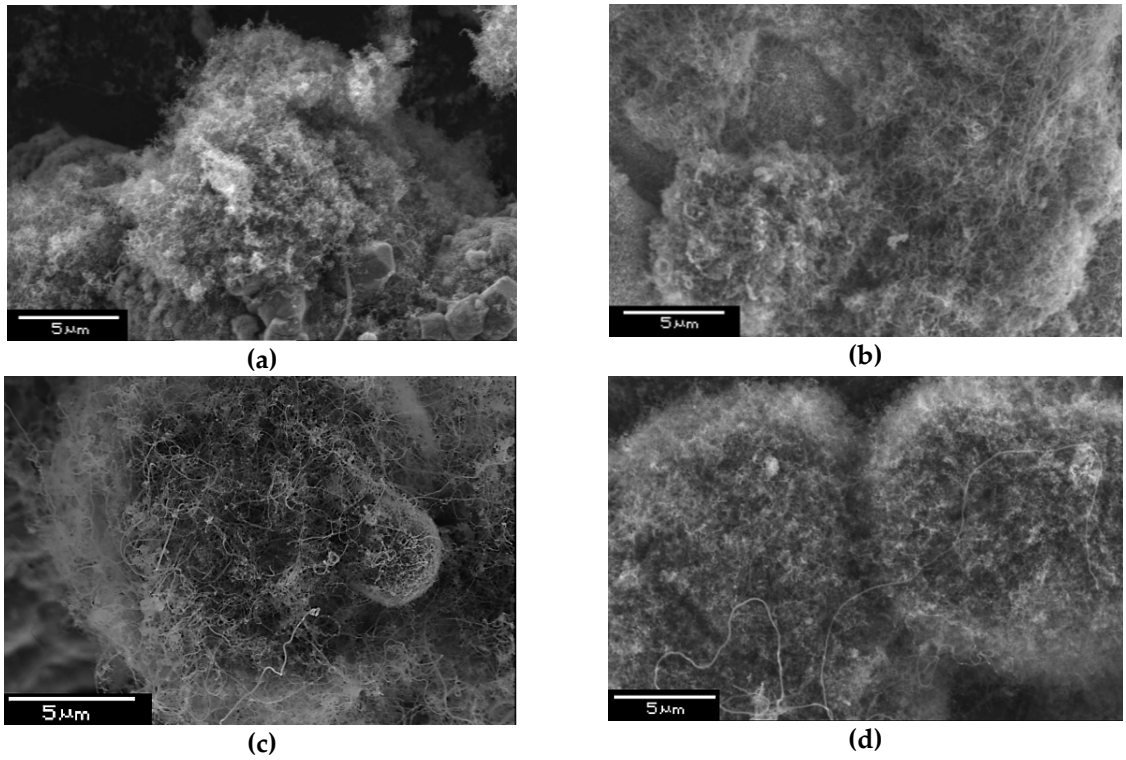

169 **Figure** 6. Microstructure of composites synthesized with Ni catalyst (**a**) and Co catalyst (**b**) (synthesis time 10
170 min) and with Ni catalyst (**c**) and Co catalyst (**d**) (synthesis time 20 min)

If we compare the dependence of weight gain with SEM images, one can see for 10 minutes samples that the structures are similar and carbon amount is approximately equal. Increasing the synthesis time to 20 minutes leads to the fact that the sample with a nickel catalyst has a higher carbon content, and the length of the carbon structures is greater. Co catalyst differs from Ni-containing one. Decontamination process in the case of cobalt occurs quicker and after 10 minutes significant weight gain is not observed. When nickel is used, the increase in carbon content is due to an increase in the fibers length (Figure 6 c,d). Next, we conducted experiments on powders with nanotubes obtained on nickel and cobalt catalysts. At equal carbon content, physical and mechanical characteristics coincided. Variation of nanotubes length must influence the physic mechanical properties, however, for our technique to achieve a big difference in length with equal contents is quite a difficult task.

At the next stage, a powder with short CNFs was selected for further mechanical activation. Mechanical activation of the powder was carried out with the aim of reinforcing the particles throughout the volume by carbon nanofibers.

Grinding was carried out under argon either without any additives or with addition of flux. Flux was added to destroy the oxide film on the surface of the original aluminum particles and to prevent significant welding of particles.

The KCl-NaCl-LiF system flux was introduced to break the oxide film on the aluminum surface during the grinding process. We used Al powder with 2.5±0.2 wt % CNFs content.

The results are shown in Figure 7. Particles up to 500 μm in size that have almost spherical shape were obtained without flux. With the flux particle size is less than 200 microns and has a plate-like shape.

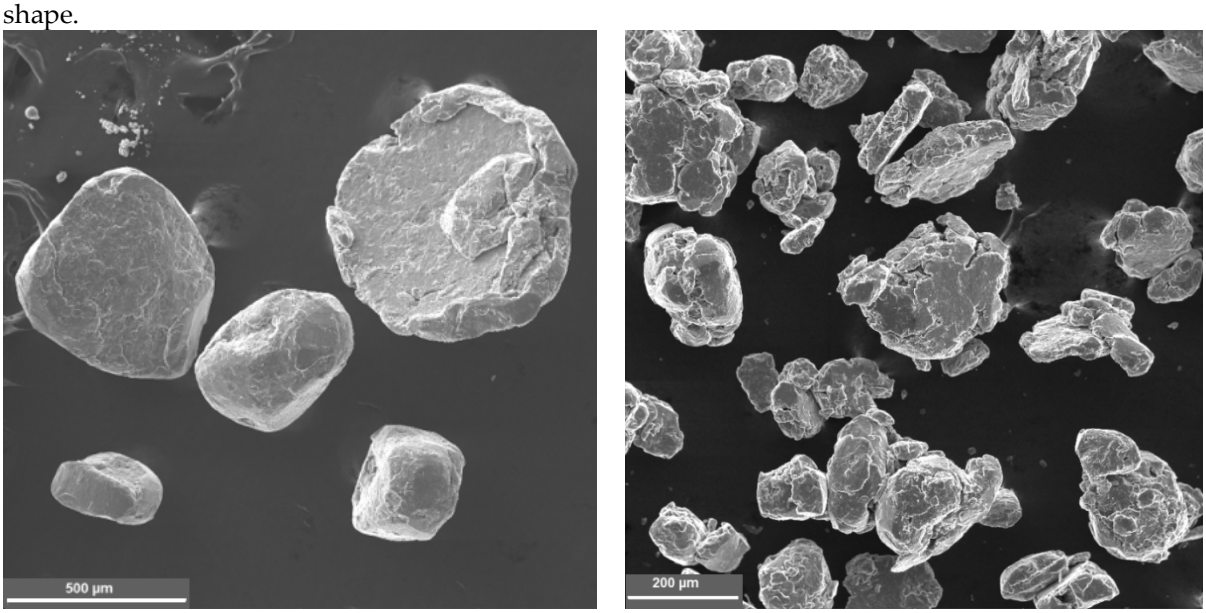

(**a**) (**b**)

Figure 7. Microstructure of composites after treatment in a planetary mill

After treatment in a planetary mill, the particles have a coarse morphology and a size of 50-200 μm (Fig 6(a)). Investigation of the microstructure of the composite particles shows a good carbon distribution (Fig 7(b)). The microhardness of particles was 200 HV (microhardness of the particles mechanically activated without flux was 100-120 HV). A significant increase in hardness when using flux can be explained by the formation of stronger bond between the CHFs and aluminum due to oxide film removal.

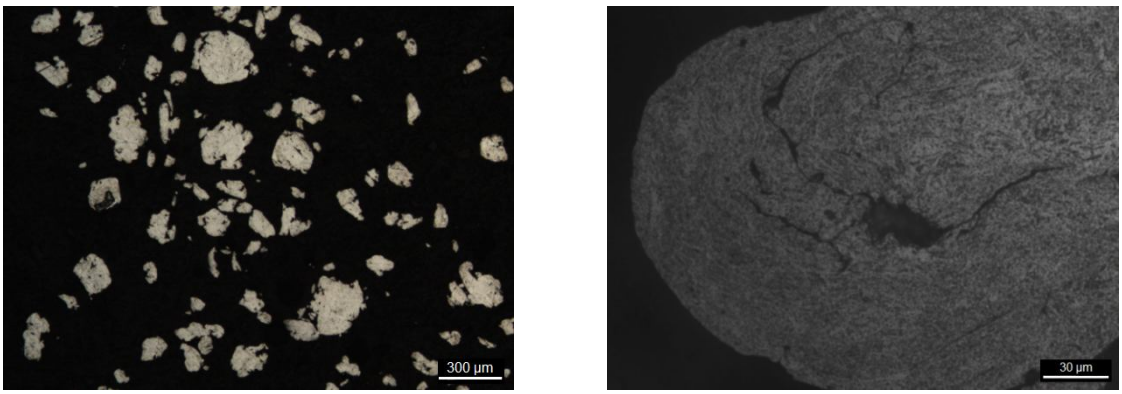

(**a**) (**b**)

Figure 8. Structural characteristics of the composite particle microstructure.

Powder material after mechanical activation with flux was compacted by the hot pressing. To vary the carbon content in this study, pure aluminum was added to the powder after the mechanical activation and mixed for additional 15 minutes under the same conditions. Thus, samples with 1 and 0.5 wt.% carbon were obtained. Hardness and thermal conductivity of materials were investigated (Figure 9). For comparison, we provide data for the specimens compressed immediately after synthesis and ones not subjected to mechanical activation [27].

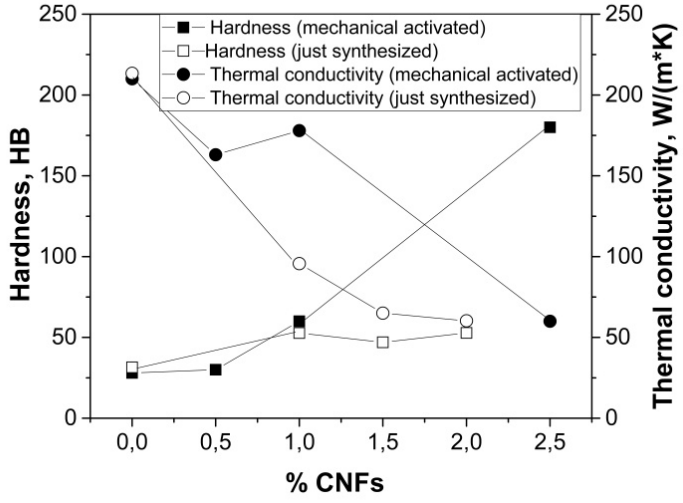

Figure 9. Hardness and thermal conductivity vs. carbon content

Hardness of the material with 2.5 wt.% CNF reached 180 HV. Its thermal conductivity was 60 W/(m·K), that corresponds approximately to the value of the specimens with 1–2 wt.% CNF without mechanic activation. These low values are explained by the appearance of a thermal barrier at the interface and by the aluminum carbide formation [27]. Dilution of the composite powder with pure aluminum leads to a hardness decrease and a sharp thermal conductivity increase. At 0.5–1% CNF, thermal conductivity of 160-180 W/(m·K) is ca. 70% from the value for pure Al (237 W(m·K) at 300 K [28]). If nanofibers are located at the surface, thermal conductivity was 96 W(m·K) at similar hardness (ca. 60 HV). The increase in thermal conductivity is due to increased Al-Al contact in the composite.

To determine the plastic characteristics, the composites were tested for bending. Figure 10(a-d) demonstrates bending tests results along with composites structures.

The composite with a uniform fine structure (Figure 10b) has a sufficiently high bending strength (485 MPa); at the same time, plasticity is practically absent. Composites diluted with pure Al (Figure10 c,d) look like grains of pure aluminum surrounded by reinforced particles. At small CNFs amount,

matrix particles are deformed and represent plates. The strength is reduced significantly down to 310 and 165 MPa for 1 and 0.5 wt%, respectively. Corresponding relative elongation was 4 and 5.8%. Low strength at a relative elongation of 5.8% (sample with 0.5 wt%) suggests that additional compacting is required by hot rolling or extrusion.

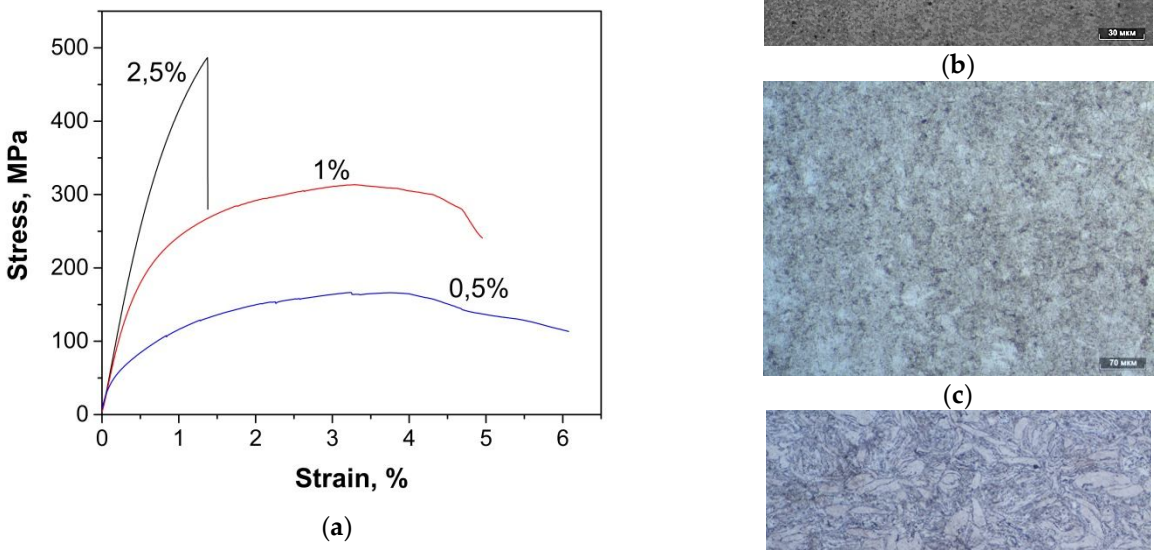

(**a**) (**b**) (**c**) (**d**)

Figure 10. The results of three point flex test of Al-CNFs composites (**a**) and optical micrographs of the polished cross sections of (**b**) 2.5 wt%, (**c**) 1 wt% and (**d**) 0.5 wt% Al –CNTs composites.

Thus, during the study we determined that the *in situ* synthesis of nanostructures and subsequent mechanical activation provides a good distribution of nanofibers and a homogeneous microstructure of the composite.

The introduction of a flux during mechanical activation contributes to the reduction of adhesion between the particles, the better reinforcement aluminum particles and the connection between the CNFs and aluminum due to the oxide film removal.

The introduction of pure aluminum particles into the mechanically alloyed powder allows varying the strength, ductility and thermal conductivity of the composite for specific applications. This approach will provide a uniform distribution of the dispersed phase in the aluminum matrix and strengthen the binding between CNF and the matrix.

4. Conclusions

The paper presents the study of the powder metallurgy production of aluminum-based composites, reinforced by carbon nanostructures with different amount of CNFs. The main conclusions are as follows:

(1) Gas phase technique for carbon nanostructures catalytic synthesis directly on the Al microparticles surfaces allows to gain uniform distribution of carbon in the matrix.

Deactivation of cobalt catalyst starts earlier than that of nickel catalyst, but with an equal carbon content, the type of catalyst does not affect the physical and mechanical characteristics.

(2) Mechanic activation provides well nanofibers distribution as well as homogeneous composite microstructure. The introduction of flux during mechanical activation helps to reduce the weldability of particles; also, better reinforcement of aluminum particles and the connection between CNFs and aluminum are reached by removing the oxide film.

(3) Strength, ductility and thermal conductivity of the composite can be varied by introducing pure aluminum in different concentrations.

Author Contributions: Andrei I. Rudskoy and Oleg V. Tolochko conceived and designed the experiments; Tatiana S. Koltsova and Elizaveta V. Bobrynina performed the experiments and analyzed the data; Elena Zemtsova, Sergey Kirichenko conducted physico-chemical studies and discussed them, Oleg V. Tolochko and Vladimir Smirnov wrote the paper.

Funding: This study was supported by the State Key Program of the National Natural Science of China (Grant No. 51734009) and by the grant of St. Petersburg State University, Event 3-2018 (id: 26520317).

Acknowledgments: The studies were performed at Research parks of St. Petersburg State University «Center for Optical and Laser Research» and «Center for Innovative Technologies of Composite Nanomaterials»

Conflicts of Interest: The authors declare no conflict of interest.

References

1. Bakshi, S.R.; Lahiri, D.; Agarwal, A. Carbon Nanotube Reinforced Metal Matrix Composites. *International Materials Reviews*. **2010**, 55(1), 41–64. DOI 10.1179/095066009X12572530170543
2. Yu, M.-F.; Laurie, O.; Dyer M.J.; Moloni K.; Kelly T.F.; Ruoff R.S. Strength and breaking mechanism of multiwalled carbon nanotubes under tensile load. *Science.* **2000,** 287, 637–640. DOI 10.1126/science.287.5453.637
3. Kim, P.; Shi, L.; Majumdar, A.; McEuen, P.L. Thermal Transport Measurements of Individual Multiwalled Nanotubes. *Phys. Rev. Lett.* **2001,** 87 (21), 215502– 1–215502-4. DOI 10.1103/PhysRevLett.87.215502
4. Chen, W.X.; Tu, J.P.; Wang, L.Y.; Gan, H.Y.; Xu, Z.D.; Zhang, X.B. Tribological application of carbon nanotubes in a metal-based composite coating and composites. *Carbon*. ***2003,*** 41, 215–222. DOI 10.1016/S0008-6223(02)00265-8
5. Tu, J.P.; Yang, Y.Z.; Wang, L.Y.; Ma, X.C.; Zhang, X.B. Tribological properties of carbon-nanotube-reinforced copper composites. *Tribol. Lett*. **2001,** 10, 225– 228. DOI 10.1023/A:1016662114589
6. He, C.; Zhao, N.; Shi, C.; Du, X.; Li, J.; Li, H.; Cui, Q. An Approach to Obtaining Homogeneously Dispersed Carbon Nanotubes in Al Powders for Preparing Reinforced Al-Matrix Composites. *Adv.Mater.* **2007**. 19, 1128–1132. DOI 10.1002/adma.200601381
7. Stein, J.; Lenczowski, B.; Anglaret, E.; Frety, N. Influence of the concentration and nature of carbon nanotubes on the mechanical properties of AA5083 aluminium alloy matrix composites. *Carbon* **2014,** 77 44–52. DOI 10.1016/j.carbon.2014.05.001
8. Liu, Z.Y.; Xiao, B.L.; Wang, W.G.; Ma Z.Y. Developing high-performance aluminum matrix composites with directionally aligned carbon nanotubes by combining friction stir processing and subsequent rolling, *Carbon.* **2013**, 62, 35–42. DOI 10.1016/j.carbon.2013.05.049
9. Jiang, L.; Li, Z.; Fan, G.; Cao, L.; Zhang, D. The use of flake powder metallurgy to produce carbon nanotube (CNT)/aluminum composites with a homogenous CNT distribution. *Carbon* **2012**, 50, 1993-1998. DOI 10.1016/j.carbon.2011.12.057
10. Wei, H.; Li, Z.; Xiong, D.-B.; Tan, Z.; Fan, G.; Qin, Z.; Zhang D. Towards strong and stiff carbon nanotube-reinforced high-strength aluminum alloy composites through a microlaminated architecture design. *Scripta Materialia*. **2014,** 75, 30-33. DOI 10.1016/j.scriptamat.2013.11.014
11. Kim, K.T.; Eckert, J.; Menzel, S.B.; Gemming, T.; Hong, S.H. Grain refinement assisted strengthening of carbon nanotube reinforced copper matrix nanocomposites. *Appl. Phys. Lett.* **2008,** 92, 121901–121903 DOI 10.1063/1.2899939

12. Cao, L.; Li, Z.; Fan, G.; Jiang, L.; Zhang, D.; Moon, W.J.; et al., The growth of carbon nanotubes in aluminum powders by the catalytic pyrolysis of polyethylene glycol. *Carbon* **2012**, 50, 1057–1062. DOI 10.1016/j.carbon.2011.10.011
13. Yang, X.; Liu, E.; Shi, C.; He, C.; Li, J.; Zhao, N.; Kondoh K. Fabrication of carbon nanotube reinforced Al composites with well-balanced strength and ductility. *J. Alloy Comp.* **2013**, 563, 216–220. DOI 10.1016/j.jallcom.2013.02.066
14. Rudskoy, A.I.; Tolochko, O.V.; Kol'tsova, T.S.; Nasibulin, A.G. Synthesis of carbon nanofibers on the surface of particles of aluminum powder. *Metal science and heat treatment* **2014**, 55, 564-568 DOI
15. Bakshi, S.R.; Singh, V.; Balani, K.; McCartney, D.G.; Seal, S.; Agarwal, A. Carbon nanotube reinforced aluminum composite coating via cold spraying. *Surface & Coatings Technology*. **2008,** 202, 5162–5169 DOI 10.1016/j.surfcoat.2008.05.042
16. Carreno-Morelli, E.; Yang, J.; Couteau, E.; Hernadi, K.; Seo, J.W.; Bonjour, C.; Forro, L.; Schaller, R. Carbon nanotube/magnesium composites. *Phys. Status Solidi (A)*. **2004,** 201 (8), 53–R55. DOI 10.1002/pssa.200409045
17. Feng, Y.; Yuan, H.L.; Zhang, M. Fabrication and Properties of Silver-Matrix Composites Reinforced by Carbon Nanotubes. *Mater. Charact*. **2005**. 55. 211–218. DOI 10.1016/j.matchar.2005.05.003
18. So, K.P.; Jeong, J.C.; Park, J.G.; Park, H.K.; Choi, Y.H.; Noh, D.H.; Keum, D.H.; Jeong, H.Y.; Biswas, C.; Hong, C.H.; Lee,Y.H. SiC formation on carbon nanotube surface for improving wettability with aluminum *Compos. Sci. Technol*. **2013**, 74, 6. DOI 10.1016/j.compscitech.2012.09.014
19. Arai, S.; Endo, M.; Kaneko, N. Ni-deposited Multiwalled Carbon Nanotubes by Electrodeposition // *Carbon*. **2004**. 42, 641–644. DOI 10.1016/j.carbon.2003.12.084
20. Kim, K.T.; Cha, S.I.; Hong, S.H.; Hong, S.H. Microstructures and tensile behavior of carbon nanotube reinforced Cu matrix nanocomposites. *Mater. Sci. Eng., A.* **2006**. 430. 27–33. DOI 10.1016/j.msea.2006.04.085
21. Pang, L.-X.; Sun, K-N.; Ren, S.; Sun, C.; Fan, R-H.; Lu, Z-H. Fabrication and microstructure of Fe3Al matrix composite reinforced by carbon nanotube. *Mater. Sci. Eng., A.* **2007.** Vol. 447. P. 146–149. DOI 10.1016/j.msea.2006.11.070
22. Laha, T.; Agarwal, A.; McKechnie, T.; Seal, S. Synthesis and characterization of plasma spray formed carbon nanotube reinforced aluminum composite. *Mater. Sci. Eng., A.* **2004**. 381, 249–258. DOI 10.1016/j.msea.2004.04.014
23. Laha, T.; Agarwal, A. Effect of sintering on thermally sprayed carbon nanotube reinforced aluminum nanocomposite. *Mater. Sci. Eng., A*. **2008,** 480, 323–332 DOI 10.1016/j.msea.2007.07.047
24. Kwon, H.; Estili, M.; Takagi, K.; Miyazaki, T.; Kawasaki, A. Combination of hot extrusion and spark plasma sintering or producing carbon nanotube reinforced aluminum matrix composites. *Carbon* **2009,** 47, 570–577. DOI 10.1016/j.carbon.2008.10.041
25. Kondoh, K.; Threrujirapapong, T.; Imai, H.; Umeda, J.; Fugetsu, B. Characteristics of powder metallurgy pure titanium matrix composite reinforced with multi-wall carbon nanotubes. *Compos. Sci. Technol*. **2009**, 69, 1077–1081. DOI 10.1016/j.compscitech.2009.01.026
26. Sun, Y.; Chen, Q.; Diameter dependent strength of carbon nanotube reinforced composite *Appl. Phys. Lett.* **2009**, 95, 021901–021903.DOI 10.1063/1.3168520
27. Rudskoy, A.I.; Koltsova, T.S.; Shakhov, F.M.; Tolochko, O.V.; Mikhailov V.G. Effect of hot pressing modes on the structure and properties of an 'aluminum – carbon nanofibers' composite material. *Metal Science and Heat Treatment*. **2015**, 56, 525–530.
28. Babichev, A.P.; Babushkina N.A.; Bratkovskii A.M., Physical Quantities. A Handbook [in Russian], Énergoatomizdat, Moscow, Russia, 1991, 1232 p.